Structure of the A-Form and B-Form of DNA from Deuterium NMR Line Shape Simulation†

Alexander A. Nevzorov, Stephan Moltke, and Michael F. Brown*

Contribution from the Department of Chemistry, University of Arizona, Tucson, Arizona 85721

Received October 3, 1997

Abstract: Simulation of experimental solid-state deuterium (^{2}H) NMR spectra of nucleic acid fibers allows one to deduce important microscopic information about the orientation of the base pairs and the helix axis disorder. However, existing interpretations of the ^{2}H NMR spectra of Na−DNA at low humidity are not in complete agreement with the X-ray results. Here we have successfully explained ^{2}H NMR spectra of oriented films of both Li−DNA and Na−DNA with the purine bases specifically deuterated at position C8. The transformation of the coupling tensor from the principal axis system to the laboratory frame has been expanded into four subtransformations, including the crystallographically defined base plane tilt and roll angles. Alternative treatments in terms of noncollective or collective helix axis disorder are considered, and the appropriate powder-pattern limits are recovered. The ^{2}H NMR spectral line shapes have been calculated by using the Monte Carlo method, i.e., by randomly sampling over the static uniaxial distributions of the base pairs and helix axes. The results of the simulations and the structural parameters are in excellent agreement with X-ray diffraction studies, which indicate the presence of either the A-form or B-form of DNA under the given experimental conditions. Only a static distribution of base pairs is needed to account for the spectral line shapes on the ^{2}H NMR time scale, whereas the effects of faster librational motions are contained in the intrinsic line widths and the effective coupling constants. The present ^{2}H NMR approach can aid in developing a more comprehensive picture of DNA conformation and dynamics as an adjunct to X-ray crystallography, fluorescence depolarization, and light-scattering methods, and moreover may prove useful in studies of protein−nucleic acid interactions.

Introduction

Investigation of the structure and dynamics of DNA has played a central role in molecular biology and continues to do so with the development of modern molecular genetics techniques. X-ray diffraction methods have been most widely used in studies of DNA, and have led to the identification of three major forms, referred to as A-, B-, and Z-DNA.[1] The application of optical methods such as fluorescence depolarization[2] and dynamic light scattering[3] as well as NMR methods has provided important additional information regarding DNA microstructure and dynamics. Multidimensional NMR methods have been used to investigate small oligonucleotide duplexes, which has made it possible to determine their time-averaged structure by using NMR distance constraints.[4] In addition, solid-state NMR studies of DNA, in particular deuterium (^{2}H) NMR spectroscopy, have been valuable in elucidating further details of the structure and dynamics of DNA in the solid state.[5−11] Here the angular information is directly accessible through the orientation of the electric field gradient (EFG) tensor corresponding to the individual C−^{2}H bonds. Comparison of the experimental line shapes with theory allows one to determine the bond angles and orientations of the base pairs with respect to the helix axis.[7,8] In previous work, it has been shown that the ^{2}H NMR spectra of Li−DNA (the B-form) can be simulated by assuming a uniaxial distribution of the base pairs around the helix axis, including pre-averaging of the transition frequencies due to librations of the base pairs,[8] which leads to a reduction of the coupling constant due to base plane fluctuations.[6] However, the more complex ^{2}H NMR spectra of calf thymus Na−DNA (75% relative humidity) have been more difficult to explain satisfactorily.[7] When the average helix axis is oriented parallel to the main magnetic field, the Na−DNA spectrum consists of two doublets, with broad inner peaks and sharp outer peaks, which have been interpreted by assuming a superposition of contributions from both the A- and B-forms.[6,7] However, according to X-ray diffraction, only the A-form of DNA is detected under these conditions, which is inconsistent with the ^{2}H NMR interpretation. In the present work we have

† Abbreviations used: DNA, deoxyribonucleic acid; EFG, electric field gradient tensor; EtOH, ethanol; NMR, nuclear magnetic resonance; PAS, principal axis system; rh, relative humidity.

(1) Saenger, W. *Principles of Nucleic Acid Structure*; Springer-Verlag: New York, 1984.
(2) Thomas, J. C.; Allison, S. A.; Appellof, C. J.; Schurr, J. M. *Biophys. Chem.* **1980**, *12*, 177−188.
(3) Lin, S. C.; Thomas, J. C.; Allison, S. A.; Schurr, J. M. *Biopolymers* **1981**, *20*, 209−230.
(4) James, T. L. In *Encyclopedia of Nuclear Magnetic Resonance*; Grant, D. M., Harris, R. K., Eds.; Wiley: New York, 1996; Vol. 5, pp 3320−3332.
(5) Vold, R. R.; Brandes, R.; Tsang, P.; Kearns, D. R.; Vold, R. L.; Rupprecht, A. *J. Am. Chem. Soc.* **1986**, *108*, 302−303.
(6) Shindo, H.; Hiyama, Y.; Roy, S.; Cohen, J. S.; Torchia, D. A. *Bull. Chem. Soc. Jpn.* **1987**, *60*, 1631−1640.
(7) Brandes, R.; Vold, R. R.; Kearns, D. R.; Rupprecht, A. *Biopolymers* **1988**, *27*, 1159−1170.
(8) Brandes, R.; Vold, R. R.; Kearns, D. R.; Rupprecht, A. *J. Mol. Biol.* **1988**, *202*, 321−332.
(9) Brandes, R.; Vold, R. R.; Kearns, D. R.; Rupprecht, A. *Biochemistry* **1990**, *29*, 1717−1721.
(10) Alam, T. M.; Drobny, G. P. *Chem. Rev.* **1991**, *91*, 1545−1590.
(11) Vold, R. R. In *Encyclopedia of Nuclear Magnetic Resonance*; Grant, D. M., Harris, R. K., Eds.; Wiley: New York, 1996; Vol. 5, pp 3314−3320.

S0002-7863(97)03461-6 CCC: $15.00
Published on Web 04/30/1998

addressed this issue by introducing a model which accounts for the detailed DNA geometry, and includes a realistic treatment of the helix axis disorder. The ^{2}H NMR line shapes of both the A- and B-forms of DNA[5,7,8,12] are successfully described in agreement with the X-ray results. Moreover, these studies reveal structural insights which may provide a valuable source of information in future studies of DNA microstructure and its interactions with proteins.

Theory and Model

The ^{2}H NMR transition frequencies for a particular C$-^2$H bond are given by[13]

$$\nu_Q^{\pm} = \pm\frac{3}{4}\chi\left\{D_{00}^{(2)}(\Omega_{XL}) - \frac{\eta}{\sqrt{6}}[D_{-20}^{(2)}(\Omega_{XL}) + D_{20}^{(2)}(\Omega_{XL})]\right\} \quad (1)$$

where the subscript X $\equiv$ P, I denotes the frame associated with the principal axis system (P) of the *static* electric field gradient tensor or the intermediate (I) frame of the *residual* EFG tensor (i.e., leftover from motions fast on the ^{2}H NMR scale) and L denotes the laboratory frame defined by the external main magnetic field. In eq 1, $\chi \equiv \chi_Q$ or χ_Q^{eff} is the static or residual (effective) quadrupolar coupling constant and $\eta \equiv \eta_Q$ or η_Q^{eff} is the asymmetry parameter of the EFG tensor, where $0 \le \eta \le 1$. The coupling parameters χ and η are related to the principal values of the EFG tensor and can be determined from the powder-type ^{2}H NMR spectrum of unoriented DNA fibers,[12] for which the bond directions are isotropically distributed. For instance, comparison of the residual values χ_Q^{eff} and η_Q^{eff} to the appropriate static values χ_Q and η_Q yields information about the influences of pre-averaging due to fast librational motions.[11] In the above formula $D_{n0}^{(2)}(\Omega_{XL})$, where $n = 0$ or ±2, are the Wigner rotation matrix elements which define the transformation of the EFG tensor from its static or residual principal axis system, associated with a particular C$-^2$H bond of the nucleic acid base, to the laboratory frame as given by the Euler angles Ω_{XL}. Here the Rose[14] convention for body-fixed right-handed rotations is used, with the Rose[14] convention for the Wigner rotation matrices. The above transformation can be expanded into various intermediate transformations which include the orientation of the C$-^2$H bond with respect to the ring system of the base, the orientation of the base plane, including the roll and tilt angles with respect to the helix axis, the distribution of the helix axes, and the orientation of the sample as a whole with respect to the external magnetic field.

In general, there are two strategies for simulating solid-state NMR spectra, e.g., involving quadrupolar, dipolar, or chemical shift interactions. The first is to derive a closed-form line shape function, which is limited to fairly simple distributions, such as spherical or cylindrical powder-type averaging.[15,16] For a simple distribution of a C$-^2$H or C$-$C^{2}H$_3$ bond on a cone, the closed-form expression for the ^{2}H NMR line shape in the case of an axially symmetric EFG tensor has also been derived.[16−18] Alternatively one can consider jump-type models.[10,19−21] However, in the more complex case of DNA, which involves an asymmetric EFG tensor, analytical derivation of the line shape function represents a difficult mathematical task. This is due to the fact that multiple subtransformations are needed to account for the complicated DNA geometry, including the base pair tilt and roll, and the DNA helix disorder. Therefore, an alternative is to simulate numerically the line shape by either summing over the contributions from all possible angles weighted with an appropriate probability density[6−8,10,17] or randomly sampling over the angles in accordance with their distribution functions to accumulate the spectrum (Monte Carlo line shape simulation).[22] The latter approach proves to be more suitable when the geometry of the system becomes more complicated and involves static distributions of more than one parameter.

In one existing model, herein referred to as model I, the DNA geometry is approximated by introducing two subtransformations.[8] Namely, the matrix elements $D_{n0}^{(2)}(\Omega_{XL})$ can be expanded in the following way:

$$D_{n0}^{(2)}(\Omega_{XL}) = \sum_{m=-2}^{2} D_{nm}^{(2)}(\Omega_{XF})\, D_{m0}^{(2)}(\Omega_{FL}) \quad (2)$$

The first set of Euler angles $\Omega_{XF} \equiv (0, \pi/2 - \theta_T, \phi_{TW} + \phi_H)$ includes the base plane tilt (θ_T) and twist (ϕ_{TW}) angles, where ϕ_H is the angle of the base plane rotation around the helix axis, and the second set is given by $\Omega_{FL} \equiv (0, \alpha, 0)$, where α describes the helix orientation within a DNA fiber or film as a whole with respect to the main magnetic field. To take into account the effects of dynamical pre-averaging, eq 2 can be integrated from $(\pi/2 - \bar{\theta}_T) - \theta_0$ to $(\pi/2 - \bar{\theta}_T) + \theta_0$ with respect to θ_T, and from $\bar{\phi}_{TW} - \phi_0$ to $\bar{\phi}_{TW} + \phi_0$ with respect to ϕ_{TW} about $\bar{\phi}_{TW} = 0$, where θ_0 and ϕ_0 denote librational tilt and twist amplitudes, respectively,[8] and then divided by the normalization factor $4\theta_0\phi_0$. As can be seen, model I contains quantitative information about the librational amplitudes and base plane tilt angle, which can be obtained from the line shape simulation, while the DNA geometry and dynamics are treated in a relatively simple manner.

In the present work we consider in more detail the microscopic DNA structure and the DNA helix distribution. We thus expand the matrix elements $D_{n0}^{(2)}(\Omega_{XL})$ using closure[16] into a set of four subtransformations, depicted in Figure 1 and referred to as model II, namely

$$D_{n0}^{(2)}(\Omega_{XL}) = \sum_{m=-2}^{2}\sum_{m'=-2}^{2}\sum_{m''=-2}^{2} D_{nm}^{(2)}(\Omega_{XB}) \times D_{mm'}^{(2)}(\Omega_{BH})\, D_{m'm''}^{(2)}(\Omega_{HF})\, D_{m''0}^{(2)}(\Omega_{FL}) \quad (3)$$

Here we start with the orientation of the principal axis system (PAS) with its *z*-axis along the C8$-^2$H bond, the *y*-axis lying

(12) Brandes, R.; Vold, R. R.; Vold, R. L.; Kearns, D. R. *Biochemistry* **1986**, *25*, 7744−7751.
(13) Brown, M. F.; Chan, S. I. In *Encyclopedia of Nuclear Magnetic Resonance*; Grant, D. M., Harris, R. K., Eds.; Wiley: New York, 1996; Vol. 2, pp 871−885.
(14) Rose, M. E. *Elementary Theory of Angular Momentum*; Wiley: New York, 1957.
(15) Seelig, J. *Q. Rev. Biophys.* **1977**, *10*, 353−418.
(16) Brown, M. F. In *Biological Membranes. A Molecular Perspective from Computation and Experiment*; Merz,K. M., Roux, B., Eds.; Birkhäuser: Boston, 1996; pp 175−252.
(17) Hentschel, R.; Silescu, H.; Spiess, H. W. *Polymer* **1981**, *22*, 1516−1521.
(18) Ulrich, A. S.; Watts, A. *Solid State Nucl. Magn. Reson.* **1993**, *2*, 21−36.
(19) Wittebort, R. J.; Olejniczak, E. T.; Griffin, R. G. *J. Chem. Phys.* **1987**, *86*, 5411−5420.
(20) Greenfield, M. S.; Ronemus, A. D.; Vold, R. L.; Vold, R. R. *J. Magn. Reson.* **1987**, *72*, 89−107.
(21) Griffin, R. G.; Beshah, K.; Ebelhäuser, R.; Huang, T. H.; Olejniczak, E. T.; Rice, D. M.; Siminovich, D. J.; Wittebort, R. J. In *The Time Domain in Surface and Structural Dynamics*; Long, G. J., Grandjean, F., Eds.; Kluwer Academic Publishers, 1988; pp 81−105.
(22) Nevzorov, A. A.; Moltke, S.; Shumway, J. A.; Brown, M. F. *Proceedings of the 214th ACS National Meeting*, Las Vegas, NV, 1997.

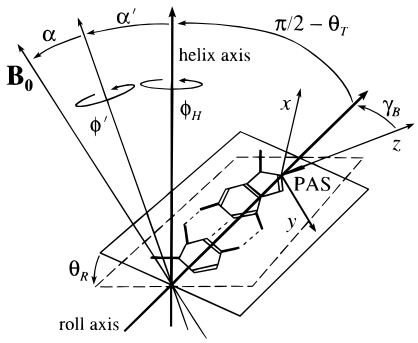

Figure 1. Transformation of the coupling tensor from the principal axis system to the laboratory frame. Here the DNA geometry is described by four transformations in agreement with the crystallographic notation. The first set of Euler angles $\Omega_{XB} \equiv (-\pi/2, \gamma_B, \theta_R)$ describes the orientation of the principal axis system (PAS) of the static (X = P) or residual (X = I) EFG tensor with respect to the roll axis of the base pair plane; the angle γ_B denotes the angle between the C$-^2$H bond and the roll axis, and θ_R is the base pair roll angle. The second set $\Omega_{BH} \equiv (\pi/2, \pi/2 - \theta_T, \phi_H)$ describes the orientation of the base pair plane with respect to the DNA helix axis, where θ_T is the tilt angle and the uniaxial distribution of the base tilt axes relative to the local helix axis is given by the angle ϕ_H. The third transformation $\Omega_{HF} \equiv (0, \alpha', \phi')$ corresponds to the uniaxial distribution of the local helix axes with respect to the average helix axis within the DNA fiber or film as given by the angles α' and ϕ'. Finally, the fourth transformation $\Omega_{FL} \equiv (0, \alpha, 0)$ describes the sample inclination (tilt) relative to the external magnetic field $\mathbf{B}_0$.

in the base plane, and consequently the *x*-axis being perpendicular to the base plane (Figure 1), which is in agreement with eq 1. The first set of Euler angles $\Omega_{XB} \equiv (-\pi/2, \gamma_B, \theta_R)$ thus pertains to the orientation of the PAS of the static or residual EFG tensor associated with the average orientation of the C$-^2$H bond with respect to the roll axis of the base pair plane;[1] the angle γ_B denotes the angle between the C$-^2$H bond and the roll axis, and θ_R is the base pair roll angle (cf. Figure 1). The second set of Euler angles $\Omega_{BH} \equiv (\pi/2, \pi/2 - \theta_T, \phi_H)$ describes the orientation of the base pair plane with respect to the DNA helix axis, taking into account the base pair tilt angle θ_T and the uniaxial distribution of the base tilt axes relative to the local helix axis, as given by the angle ϕ_H. The third transformation $\Omega_{HF} \equiv (0, \alpha', \phi')$ corresponds to the uniaxial distribution of the *local* helix axes with respect to the *average* helix axis of the DNA fiber or film as given by α' and ϕ'. Finally, the fourth transformation $\Omega_{FL} \equiv (0, \alpha, 0)$ describes the sample inclination (tilt) relative to the external magnetic field. Note that model I can be reproduced as a limiting case from model II by collapsing the first three subtransformations involving $\mathbf{D}^{(2)}(\Omega_{XB})$, $\mathbf{D}^{(2)}(\Omega_{BH})$, and $\mathbf{D}^{(2)}(\Omega_{HF})$ into one effective transformation, $\mathbf{D}^{(2)}(\Omega_{XF})$. This involves setting $\gamma_B = \theta_R = 0$ where $\bar{\phi}_{TW} = 0$, and eliminating the explicit dependence of the helix axis disorder; i.e., $\alpha' = \phi' = 0$.

Inserting eq 3 into eq 1, one can then simulate the ^{2}H NMR line shape for model II in the following simple manner, referred to as Monte Carlo line shape simulation. First a random triple of the angles ϕ_H, α', and ϕ' is generated, then the corresponding quadrupolar splitting is calculated, and finally a unit intensity is assigned for this splitting. The analogous procedure can also be applied to model I, eq 2. Uniform distributions from 0 to 2π are assumed for the angles ϕ_H and ϕ'. Values of α' are generated in the following way: random values of the distribution function of α', $P(\alpha')$, are generated from 0 to 1, and then the corresponding values of α' are calculated. The distribution function for the helix disorder $P(\alpha')$ is discussed in the next section. The other angles, such as the bond angle γ_B, the roll angle θ_R, and the tilt angle θ_T constitute the fitting parameters of the model and correspond to a particular DNA structure, such as the A- or B-form. The starting values for the parameters can be obtained from the literature.[1] Final refinement of the theoretical spectrum involves the introduction of small static distributions of the angles θ_R and θ_T and convolution of the spectral distribution with the intrinsic line shape. The spectrum can thus be easily simulated on a desktop computer. A total of about 100 000 random samples is sufficient to accumulate a smooth line shape within the spectral range of ±200 kHz.

Treatment of Helix Axis Disorder

The most widely used expression for the probability distribution involves a Gaussian probability density function, which approximates the disorder in a general fashion

$$p(\alpha') \propto \exp\left[-\frac{\alpha'^2}{2\sigma(\alpha')^2}\right] \tag{4}$$

Modifications of the normal distribution have been also proposed,[10] in which the total probability density is written as a sum of a highly oriented and highly disordered fraction of helices. In the uniaxial three-dimensional case, the probability density function should be weighted by the sine of the angle corresponding to a given axis inclination, which seems most appropriate for the description of noncollective disorder, i.e., when the axis orientations are distributed independently of one another. One example involves the case of the uniaxial disorder of immobile integral membrane proteins (mosaic spread).[23] The Gaussian probability of finding an axis orientation between α' and $\alpha' + d\alpha'$ then has an additional weight, proportional to the area element $\sin \alpha' \, d\alpha'$ on a unit sphere, which in turn implies that the probability of a perfect alignment with the average axis is zero, increasing with tilt away from the perfect orientation. However, in the case of thin films of DNA prepared by the wet-spinning method,[24,25] one deals with a *two-dimensional disorder* which would imply that the additional sine factor is not needed to describe the orientations of the DNA helix axes within a given plane. To take into account the helix disorder in the simpler model I, one needs to convolute the spectra calculated at various values of $\alpha \rightarrow \alpha \pm \alpha'$ with a Gaussian distribution centered at $\alpha' = 0$. Note that this approach is valid strictly for model I only in the case of two-dimensional disorder, and an additional subtransformation, containing explicitly the colatitude angle α' and the azimuthal angle ϕ', should be included to treat three-dimensional disorder as in model II; cf. eq 3.

As an alternative to the above formulation for the noncollective helix axis disorder, one can consider possible orientations within an entire DNA molecule, referred to as collective disorder, which also seems applicable for macroscopically oriented DNA films. Here a portion of the DNA molecule with its own axis orientation belongs to the entire molecule; cf. Figure 2. In this case the sine weighting factor for the distribution of α' is also not needed, since the uniaxial angle ϕ' rotates all the orientations of the DNA around the molecular axis at the same time. It should be noted that, in principle, one could incorporate both types of distributions by introducing a fifth transformation into model II, eq 3. However, detection of such complex

(23) Moltke, S. et al. Manuscript in preparation.
(24) Rupprecht, A. *Acta Chem. Scand.* **1966**, *20*, 494−504.
(25) Rupprecht, A. *Biotechnol. Bioeng.* **1970**, *12*, 93−121.

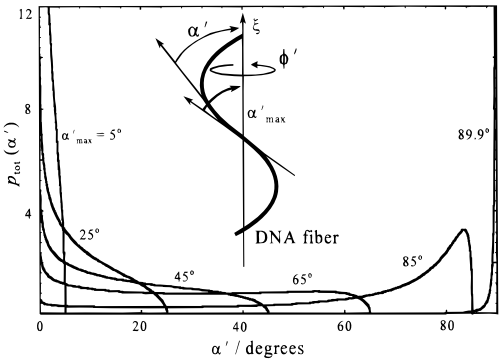

Figure 2. Probability distribution for the helix disorder as a function of the cutoff parameter α'_{max}, plotted from 5° to 85° in intervals of 20°, and at 89.9°. When $\alpha'_{max} < 50°$, the probability distribution has a sharp peak corresponding to the 0° orientation and a broad shoulder extending to larger angles, suggesting the presence of both highly ordered and relatively disordered fractions. At larger cutoffs the maximum asymptotically shifts to 90°.

disorder from the line shape simulation would probably lie beyond the capabilities of one-dimensional solid-state ^{2}H NMR spectroscopy. Therefore, in the present paper we shall use only one type of distribution for a particular simulation and then compare the results.

In what follows we describe a simple way of treating collective disorder of the DNA helix axes. For a sample of macroscopically oriented DNA molecules, one may assume that a DNA molecule behaves as a stiff wormlike chain having a rather long persistence length, which is still substantially less than the total molecular length. One can, therefore, treat deviations of the local helix axes from the average molecular axis in terms of elementary wavelike disturbances such as cos ($k\xi$). Here ξ is the variable corresponding to length, and k is the disorder "wavevector" related to the inverse persistence length; cf. Figure 2. The orientation of an element of the DNA molecule with respect to the average molecular axis can then be calculated as

$$\tan \alpha' = \frac{d}{d\xi}(\cos k\xi) = -k \sin k\xi \tag{5}$$

If ξ is assumed to be distributed uniformly from 0 to π/k, where the cosine function is single-valued, then $p(\xi) = k/\pi$, and differentiating eq 5, the probability density for α' can be written as

$$p(\alpha') = p(\xi)\frac{d\xi}{d\alpha'} = -\frac{1}{\pi}\frac{1 + \tan^2 \alpha'}{(k^2 - \tan^2 \alpha')^{1/2}} \tag{6}$$

The total probability density function can then be obtained by integrating over the range of k in eq 6 where the integral exists, i.e., from $k_{min} \equiv \tan \alpha'$ up to a maximum cutoff value $k_{max} \equiv \tan \alpha'_{max}$. The result is

$$p_{tot}(\alpha') = \frac{N}{\cos^2 \alpha'}\int_{\tan \alpha'}^{\tan \alpha'_{max}} \frac{dk}{(k^2 - \tan^2 \alpha')^{1/2}} = \frac{N}{\cos^2 \alpha'} \operatorname{sech}^{-1}\left(\frac{\tan \alpha'}{\tan \alpha'_{max}}\right) \tag{7}$$

where N is a normalization constant, $N = (\pi/2 \tan \alpha'_{max})^{-1}$. The corresponding (cumulative) distribution function now becomes

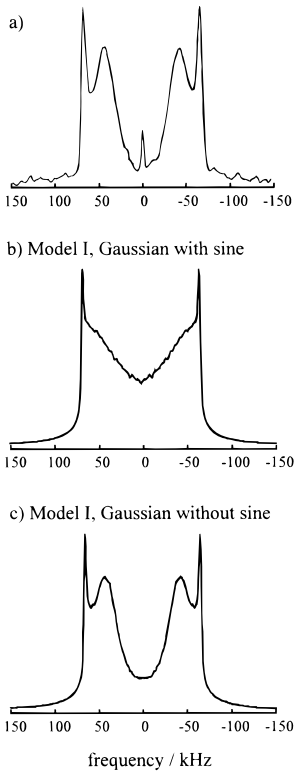

Figure 3. Simulation of ^{2}H NMR spectra of oriented films of Na−DNA at 75% relative humidity: (a) experimental ^{2}H NMR spectrum taken at 0° sample tilt angle, ref 7; (b) comparison to model I, eq 2, assuming a Gaussian distribution for the noncollective helix disorder with a sine weighting factor (three-dimensional distribution); (c) comparison to model I using a Gaussian distribution without the sine factor (two-dimensional distribution). A Gaussian line broadening of 0.6 kHz together with a correction, ref 38, for the finite pulse width of 2.5 μs has been applied for this and subsequent figures. (The use of Lorentzian line broadening yields little difference in spectral appearance.) At a sufficiently large value of $\sigma(\alpha')$ of 11° or greater, model I yields sharp outer peaks in the Na−DNA ^{2}H NMR spectrum, corresponding to a contribution from the perpendicular orientations of the C−^{2}H bonds with respect to the main magnetic field. Note that no assumption about the presence of a B-DNA fraction is necessary, which is in agreement with X-ray results. The use of the two-dimensional distribution improves the quality of the fit, which would imply that the sine weighting factor is not needed to describe helix axis disorder in planar DNA films.

$$P_{tot}(\alpha') = \int_0^{\alpha'} p_{tot}(\alpha'')\, d\alpha'' = \frac{2}{\pi}\left[\sin^{-1}\left(\frac{\tan \alpha'}{\tan \alpha'_{max}}\right) + \frac{\tan \alpha'}{\tan \alpha'_{max}} \operatorname{sech}^{-1}\left(\frac{\tan \alpha'}{\tan \alpha'_{max}}\right)\right] \tag{8}$$

Plots of the probability density function $p_{tot}(\alpha')$ for different maximum cutoffs α'_{max} are presented in Figure 2. One can see that at $\alpha'_{max} < 50°$ one has a sharp peak at zero orientation with a wide base, which is analogous to the distribution given elsewhere,[10] suggesting the presence of highly oriented and disordered fractions of the helix axes, but described by only one parameter, α'_{max}. At larger cutoffs the maximum asymptotically shifts to 90°; cf. Figure 2.

Simulation of Lithium and Sodium DNA ^{2}H NMR Spectra

For this work we have relied on published ^{2}H NMR spectra of calf thymus Na−DNA (75% relative humidity) and Li−DNA

Table 1. Summary of Parameters of Models I and II Used To Simulate ^{2}H NMR Spectra of the A-Form and B-Form of DNA

parameter	Li−DNA (66% rh)	Na−DNA (75% rh)	Na−DNA (1% excess NaCl, EtOH treated, 66% rh)	Na−DNA (1% excess NaCl, EtOH treated, 75% rh)
	Model I			
coupling constant, χ_Q/kHz	179	179	179	179
asymmetry parameter, η_Q	0.06	0.06	0.06	0.06
base tilt angle, $\bar{\theta}_T \pm \sigma(\theta_T)$/deg[a]	-6 ± 3	22.5 ± 3	22.5 ± 3	22.5 ± 3
tilt librational amplitudes, θ_0/deg	10	10	10	10
twist librational amplitudes, ϕ_0/deg	12	12	12	12
noncollective helix axis disorder with sine factor (3-D), $\sigma(\alpha')$/deg[a]		11		
noncollective helix axis disorder without sine factor (2-D), $\sigma(\alpha')$/deg[a]		16.5	14	12
	Model II			
coupling constant, χ_Q^{eff}/kHz[b]	173	173	173	173
asymmetry parameter, η_Q^{eff} [b]	0.065	0.065	0.065	0.065
C8−C1′ bond angle, γ_B/deg[c]	13	13	13	13
base roll angle, θ_R/deg	−4	6	6	6
base tilt angle, $\theta_T \pm \sigma(\theta_T)$/deg[a]	-6 ± 3	21.5 ± 3.7	21.5 ± 3.7	21.5 ± 3.7
cutoff for the collective distribution of helix axes, α'_{max}/deg	30	34	27	26

[a] Assuming a Gaussian distribution. [b] Average values determined from simulation of the ^{2}H NMR powder-type spectrum of Li−DNA, ref 12. [c] Obtained from the base pair geometry given in ref 1.

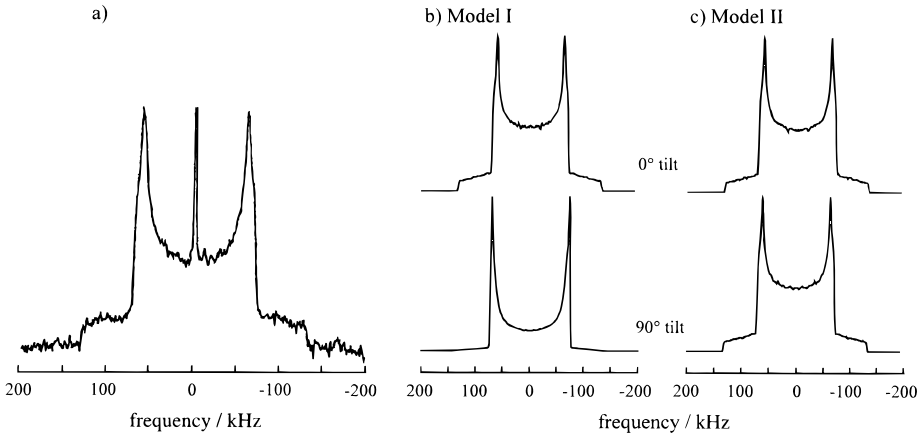

Figure 4. Simulation of the ^{2}H NMR powder-type spectrum of Li−DNA at 66% relative humidity: (a) experimental ^{2}H NMR spectrum for randomly oriented Li−DNA, ref 12; (b) comparison to the powder-type limit of model I, eq 2, for 0° and 90° tilt angles; (c) comparison to the powder limit of model II, eq 3, for 0° and 90° tilt angles. Note that model I yields a powder pattern at 0° sample tilt but fails to do so at a sample tilt of 90°, which is due to the effectively two-dimensional character of the helix disorder considered by the model. The more detailed model II, which considers three-dimensional uniaxial helix disorder, yields a powder-type spectrum as a limiting result at all tilt angles. The coupling parameters χ_Q^{eff} and η_Q^{eff} used in the simulation of the experimental ^{2}H NMR spectrum are given in Table 1.

(66% relative humidity), both having specifically deuterated purine rings at position C8.[5,7,8,12] A Monte Carlo line shape simulation method was used to simulate the experimental ^{2}H NMR spectra of DNA in order to avoid mathematical and computational difficulties associated with the direct derivation of an analytical expression. All calculations were performed on a desktop computer operating at 100 MHz using MATLAB (The MathWorks, Inc., Natick, MA).

A representative ^{2}H NMR spectrum of Na−DNA at zero sample inclination (tilt)[7] is shown in part a of Figure 3. As can be seen, the spectrum contains two relatively broad inner peaks and two sharp outer peaks. Figure 3, part b, shows the simulation of the Na−DNA ^{2}H NMR spectrum at zero sample tilt by using model I, eq 2, with a Gaussian distribution of the helix axes including the sine factor (three-dimensional noncollective disorder), with the values of the fitting parameters as reported in Table 1. However, as can be seen from comparison of parts a and b of Figure 3, the use of a Gaussian distribution of the helix axes with the sine factor gives rise to a significant excess of intensity in the spectral center, i.e., near the carrier frequency. As an alternative, model I has been used assuming a two-dimensional noncollective helix disorder, i.e., a Gaussian distribution without the sine factor with the fitting parameters summarized in Table 1, which led to a significant improvement of the fit; cf. Figure 3, part c. This would seem to imply that the two-dimensional distribution of the helix axes is indeed more suitable for simulating NMR spectra of macroscopically oriented DNA films rather than a Gaussian function with a sine weighting factor.

One should note at this juncture that the above theoretical ^{2}H NMR spectra of Na−DNA can be explained in simple intuitive terms. Setting the base plane tilt angle to about 20° (that is 70° relative to the helix axis) gives rise to the quadrupolar splitting near ±45 kHz at 0° sample tilt, whereas a sufficiently large value of $\sigma(\alpha')$ of 16.5° yields the sharp outer peaks at ±60 kHz, corresponding to perpendicular orientations of the C−^{2}H bonds relative to the main magnetic field. The perpendicular component is due to the combined effect of mosaic spread of the helix axes together with the static disorder of base plane tilt and roll, which results in a fraction of the C−^{2}H bond distribution which intersects the laboratory (x, y) plane and gives rise to the characteristic 90° singularities in ^{2}H NMR spectroscopy.[16]

As a further test, model I has been used to simulate a powder-pattern ^{2}H NMR spectrum as a limiting case. Indeed, if the helix axis orientations are assumed to be distributed uniformly

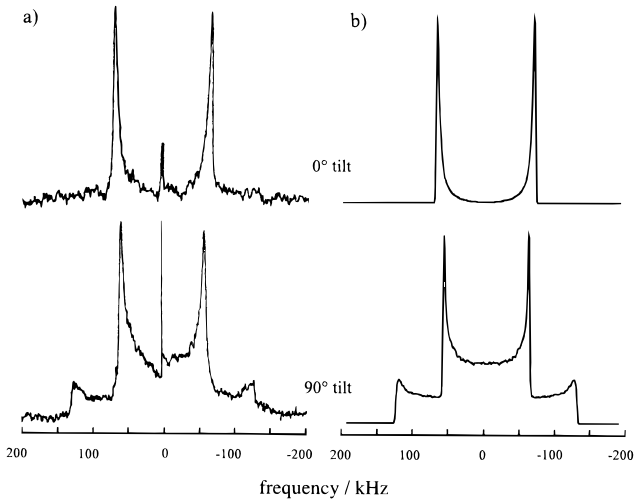

Figure 5. Simulation of ^{2}H NMR spectra of oriented films of Li−DNA at 66% relative humidity assuming collective helix axis disorder, eqs 7 and 8: (a) experimental ^{2}H NMR spectra for the B-form at 0° and 90° sample tilt angles, ref 5; (b) theoretical simulations for 0° and 90° sample tilt angles using model II with the fitting parameters summarized in Table 1. A Gaussian line broadening of 0.6 kHz together with a correction, ref 38, for the finite pulse width of 2.5 μs has been applied. The model is able to fit the experimental ^{2}H NMR spectra, and the fitting parameters are in agreement with X-ray results.

over a unit sphere, i.e., if $\alpha \rightarrow \alpha \pm \alpha'$ and cos α' is uniformly distributed from +1 to −1, then the model should yield a limiting powder-type spectrum regardless of the macroscopic tilt angle α of the sample. Figure 4, part a, shows a ^{2}H NMR powder-type spectrum of Li−DNA;[12] simulations corresponding to the powder limit of model I for sample tilt angles $\alpha = 0°$ and $\alpha = 90°$ are shown in part b, with the fitting parameters given in Table 1. As can be seen, the model generates a powder-type pattern for the 0° sample tilt, but fails to do so if the sample is tilted at 90°. The reason for this is that model I does not explicitly contain the angle ϕ', cf. eq 2, and thus effectively corresponds to a two-dimensional treatment of the helix axis disorder. By contrast, part c of Figure 4 shows that the alternative model II, eq 3, gives a typical powder pattern in both cases due to the presence of the nonvanishing azimuthal angle ϕ' describing three-dimensional orientations of the helix around its average axis, which justifies the more detailed expansion in eq 3. Note that even though additional subtransformations are considered in eq 3, the model still yields a typical powder-type spectrum, which can also be described by the simple Pake formula[15,16] in terms of a spherical powder-type average over the bond orientations Ω_{XL}. From the fit to the powder-type spectrum, the effective coupling parameters $\chi_Q^{eff} = 173$ kHz and $\eta_Q^{eff} = 0.065$ have been obtained;[12] cf. Table 1.

Figure 5 shows a comparison of the experimental ^{2}H NMR spectra of Li−DNA,[5] part a, to simulations obtained by using the more detailed model II, part b, together with the collective distribution of the helix axes as given by eqs 7 and 8, and the fitting parameters summarized in Table 1 for sample tilt angles of $\alpha = 0°$ and $\alpha = 90°$. Comparable results are obtained for model II using a Gaussian distribution without the sine factor (not shown). If the tilt angles of the base planes are set nearly perpendicular to the helix axis for 0° sample tilt, the cylindrical symmetry about the main magnetic field leads to a single quadrupolar splitting with peaks at ±60 kHz, corresponding to the B-form of DNA; cf. Figure 5. When the sample is inclined at 90°, the most probable orientation of the cylindrically-distributed base pair planes is still perpendicular to the magnetic field, giving rise to the peaks at around ±60 kHz. However,

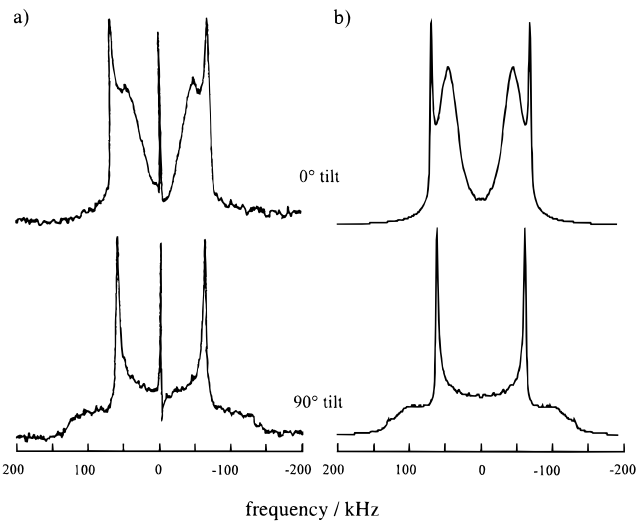

Figure 6. Simulation of ^{2}H NMR spectra of oriented films of Na−DNA at 75% relative humidity assuming collective helix axis disorder, eqs 7 and 8: (a) experimental ^{2}H NMR spectra for 0° and 90° sample tilt angles, ref 5; (b) theoretical simulations for 0° and 90° sample tilt angles using model II with the fitting parameters summarized in Table 1. A Gaussian line broadening of 0.8 kHz and a correction for the finite pulse width of 2.5 μs have been applied. Note that model II having collective helix disorder describes the data comparably to model I with noncollective helix disorder for the 0° sample tilt; cf. Figure 3.

there is also a fraction of base planes aligned parallel to the external magnetic field, which yields the additional peaks at about ±120 kHz. Note that the present model II fits the 0° tilt Li−DNA spectra as well as model I[8] assuming noncollective three-dimensional helix axis disorder. However, an obviously better quality of the fits of the 90° sample tilt spectra is observed *versus* model I,[8] and no assumption about the orientation dependence of the transverse relaxation rates[8] is necessary.

The fits of model II to the ^{2}H NMR spectra of oriented samples of Na−DNA,[5] part a of Figure 6, for sample tilt angles of $\alpha = 0°$ and $\alpha = 90°$ are shown in part b of Figure 6, and the fitting parameters are presented in Table 1. The helix axes are distributed according to eqs 7 and 8 assuming collective helix axis disorder. The same parameters describe simultaneously the ^{2}H NMR spectra of the Na−DNA helices oriented at both 0° and 90° relative to the main magnetic field; cf. Table 1. Note that model II assuming collective helix disorder gives results almost indistinguishable from those for two-dimensional helix disorder, eq 4, at 0° sample tilt, but yields rounder shoulders at 90° compared to the latter (not shown), which is more consistent with experimental data. The results for Na−DNA in Figure 6 can also be compared to those for model I with the treatment of two-dimensional noncollective helix disorder; cf. part c of Figure 3.

Finally, theoretical simulations of the ^{2}H NMR spectra of Na−DNA treated with EtOH at different relative humidities[7] are shown in Figure 7 with the fitting parameters given in Table 1. Here varying the spread of the helix axes yields different ratios of the inner to outer peak intensities. It is noteworthy that a previous interpretation[5,7] involved the assumption of a change in the A-form to B-form DNA ratio at different relative humidities. By contrast, the present model suggests that the effect of humidity and EtOH treatment mainly affects the helix disorder (mosaic spread) without changing the DNA structure. This conclusion is in full agreement with the X-ray crystallographic data which also suggest the presence of only the A-form under the given conditions.[7] Thus, the 90° singularities in the ^{2}H NMR Na−DNA spectra are most

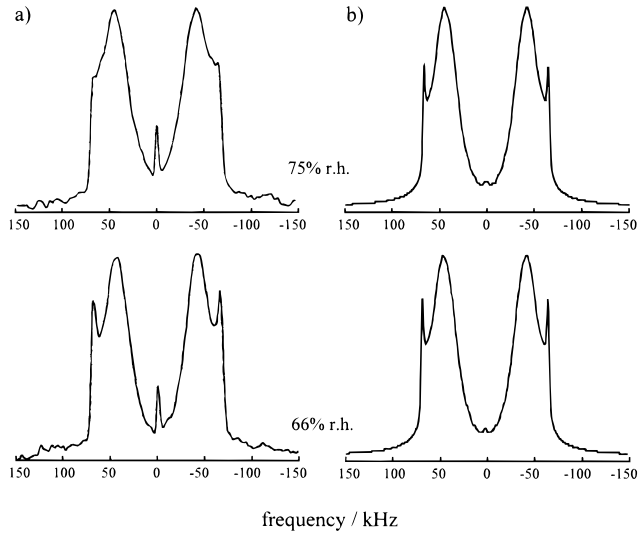

Figure 7. Simulation of ^{2}H NMR spectra of EtOH-treated Na−DNA at different relative humidities using model II: (a) experimental spectra for 75% and 66% relative humidities at 0° sample tilt angle, ref 7; (b) theoretical simulations for 0° sample tilt angle with the fitting parameters given in Table 1. The model for the collective disorder suggests that the ratio of the inner to outer peaks depends on the degree of helix disorder, and not on a change in the A- to B-form ratio.

probably due to a larger degree of helix axis disorder than that used in Brandes et al.,[7] which in addition may be sensitive to external conditions (relative humidity, salt concentration, etc.).

Discussion

It is widely recognized that deuterium (^{2}H) solid-state NMR spectroscopy constitutes a powerful tool for investigating the dynamical and equilibrium properties of the nucleic acids[5−8,10,11] in combination with X-ray crystallography,[26−28] fluorescence depolarization,[2] dynamic light scattering,[3] and multidimensional solution NMR spectroscopy.[4] In previous work,[8,12] it has been shown that the ^{2}H NMR spectra of the B-form of calf thymus DNA can be simulated by a model that approximates the base plane geometry by using two subtransformations pre-averaged over fast (on the ^{2}H NMR time scale) librational motions. However, the more complicated ^{2}H NMR spectra exhibited by the A-form of DNA have been more difficult to explain satisfactorily.[7] Under conditions where, according to X-ray diffraction, only the A-form of DNA is present (Na salt, low relative humidity),[1,29] the ^{2}H NMR spectrum reveals additional features such as sharp outer peaks. The ^{2}H NMR spectra of the Na−DNA have been previously simulated[7] under the assumption of a superposition of contributions from both the A-form and B-form of DNA, which apparently are not detectable using X-ray diffraction techniques. One should note that typically only the ordered regions of the sample are observed with X-ray diffraction, and the contribution from the diffuse background scattering is neglected. Thus, an additional aspect is whether current theoretical formulations are sufficient to accurately account for the solid-state NMR spectra of DNA films at the microscopic level in terms of the equilibrium properties as established via X-ray diffraction methods.

In this work we have addressed the correspondence of solid-state ^{2}H NMR spectroscopy to X-ray diffraction data for DNA films using a simple Monte Carlo line shape simulation method. The complex DNA geometry is described in detail by four intermediate rotational subtransformations, including either two-dimensional noncollective disorder of the average molecular axes or collective disorder within one DNA molecule. In the latter case the stiff DNA molecules are assumed to have a strong preferential average direction which allows one to treat the disorder within one molecule in terms of wavelike disturbances of a wormlike chain. Experimental ^{2}H NMR spectra of both Li− and Na−DNA have been simulated self-consistently for different sample tilt angles. The assumption about a two-dimensional character of the helix disorder yields adequate intensities of the inner and outer peaks with respect to the intensity in the center, in agreement with the experimental ^{2}H NMR spectra of Na−DNA films. Note that, in contrast to previous simulations,[6,7] no assumption about the presence of the B-form in the Na−DNA spectra is necessary, which removes previous discrepancies between the results of ^{2}H NMR spectroscopy and X-ray diffraction. Moreover, the present approach explains the effect of relative humidity mainly by changes in the helix axis disorder with water content, and not by changes in the A- to B-form ratios.[7] The values of the roll and tilt angles obtained from the line shape simulation are in good agreement with X-ray data.[1,30] A detailed treatment of the *static* disorder within the NMR frequency and temperature range studied in terms of the combined effects of the helix axis disorder and the distribution of base plane tilt and roll angles proves to be sufficient to describe the complicated ^{2}H NMR spectral features of the oriented DNA samples. In previous work[7] the effect of the helix axis disorder has been underestimated, leading to the possible misidentification of the sharper outer peaks in the 0° tilt Na−DNA spectra with the presence of the B-form, rather than as a characteristic feature of the A-form. It should be noted that an attempt to reconstruct the form of the distribution of DNA helix axes directly from the experimental ^{2}H NMR spectra has also been made (not shown), involving singular value decomposition methods.[31,32] It was found that the helix distribution could not be obtained to an acceptable accuracy from the given experimental data, which makes the choice of the model for the helix disorder somewhat arbitrary depending on the plausibility of the physical picture employed. This question may be resolved in the future with the use of deconvolution techniques for two-dimensional solid-state NMR spectra.[33,34]

As noted before, the observed DNA ^{2}H NMR line shapes can be simulated by assuming only a static distribution of the base pair orientations, thus reflecting mainly the equilibrium properties of DNA. In the present approach the possible effects from motions have been taken into account in terms of the intrinsic line widths and effective coupling constants which are related to motional amplitudes.[11] On the other hand, the convenient closure expression combined with the Monte Carlo line shape simulation makes it possible to include pre-averaged subtransformations containing the motional amplitudes instead of using the effective coupling parameters. However, since there are only two effective coupling constants, χ_Q^{eff} and η_Q^{eff}, which

(26) Wilkins, M. H. F. *Science* **1963**, *140*, 941−950.
(27) Kim, S.-H.; Quigley, G.; Suddath, F. L.; Rich, A. *Proc. Natl. Acad. Sci. U.S.A.* **1971**, *68*, 841−845.
(28) Wing, R. M.; Drew, H. R.; Takano, T.; Broka, C.; Tanaka, S.; Itakura, K.; Dickerson, R. E. *Nature* **1980**, *287*, 755−758.
(29) Cooper, P. J.; Hamilton, L. D. *J. Mol. Biol.* **1966**, *16*, 562−563.
(30) Wüthrich, K. *NMR of Proteins and Nucleic Acids*; John Wiley: New York, 1986.
(31) Pusep, A. Y.; Shokhirev, N. V. *Opt. Spectrosc.* **1984**, *57*, 482−486.
(32) Shokhirev, N. V.; Rapatskii, L. A.; Raitsimring, A. M. *Chem. Phys.* **1986**, *105*, 117−126.
(33) Tang, P.; Santos, R. A.; Harbison, G. S. *Adv. Magn. Reson.* **1989**, *13*, 225−255.
(34) Schmidt-Rohr, K.; Spiess, H. W. *Multidimensional Solid-State NMR and Polymers*; Academic Press: San Diego, 1994.

can be determined experimentally, the number of motional amplitudes used in the model cannot exceed two without being underdetermined, whereas obviously many more types of motions occur in DNA including base roll, tilt, and twist librational motions and DNA string undulations.[35,36] Therefore, at present it seems more suitable to treat the dynamical effects on ^{2}H NMR solid-state spectra of complex systems by means of effective coupling constants and line widths, leaving the specific details for NMR relaxation studies.[9,37] The solid-state ^{2}H NMR line shape method described here can aid in developing a more comprehensive picture of DNA internal structure and its interactions with proteins, and may be of interest as an adjunct to other experimental techniques, such as multidimensional high-resolution NMR spectroscopy, fluorescence depolarization, and light scattering studies.

Acknowledgment. This work was supported by the U.S. National Institutes of Health and by a postdoctoral fellowship from the Deutsche Forschungsgemeinschaft (S.M.).

JA9734612

(35) Allison, S. A.; Shibata, J. H.; Wilcoxon, J.; Schurr, J. M. *Biopolymers* **1982**, *21*, 729−762.

(36) Song, L.; Allison, S. A.; Schurr, J. M. *Biopolymers* **1990**, *29*, 1773−1791.

(37) Wang, A. C.; Kennedy, M. A.; Reid, B. R.; Drobny, G. P. *J. Am. Chem. Soc.* **1992**, *114*, 6583−6585.

(38) Bloom, M.; Davis, J. H.; Valic, M. I. *Can. J. Phys.* **1980**, *58*, 1510−1517.